2002

Nonlinear Kinematic Tolerance Analysis of Planar Mechanical Systems

Min-Ho Kyung

Elisha Sacks
Purdue University, eps@cs.purdue.edu

Report Number:
02-004

NONLINEAR KINEMATIC TOLERANCE ANALYSIS OF PLANAR MECHANICAL SYSTEMS

Min-Ho Kyung
Elisha Sacks

Department of Computer Sciences
Purdue University
West Lafayette, IN 47907

CSD TR #02-002
January 2002
(Revised May 2002)

Nonlinear kinematic tolerance analysis of planar mechanical systems

Min-Ho Kyung and Elisha Sacks (correspondent)
Computer Science Department
Purdue University
West Lafayette, Indiana 47907
Phone: 1-765-494-9026; E-mail: eps@cs.purdue.edu

Abstract

This paper presents a nonlinear kinematic tolerance analysis algorithm for planar mechanical systems comprised of higher kinematic pairs. The part profiles consist of line and circle segments. Each part translates along a planar axis or rotates around an orthogonal axis. The part shapes and motion axes are parameterized by a vector of tolerance parameters with range limits. A system is analyzed in two steps. The first step constructs generalized configuration spaces, called contact zones, that bound the worst-case kinematic variation of the pairs over the tolerance parameter range. The zones specify the variation of the pairs at every contact configuration and reveal failure modes, such as jamming, due to qualitative changes in kinematic function. The second step bounds the worst-case system variation at selected configurations by composing the zones. Case studies show that the algorithm is accurate, fast, and far superior to a prior algorithm that constructs and composes linear approximations of contact zones.

keywords: kinematics, tolerance analysis, higher pairs.
abbreviated title: Nonlinear kinematic tolerance analysis.

Submitted to *Computer Aided Design*, May 2002.

1 Introduction

This paper presents a nonlinear kinematic tolerance analysis algorithm for planar mechanical systems comprised of higher kinematic pairs. Kinematic tolerance analysis estimates the variation in the kinematic function of systems due to manufacturing variation in part shapes and configurations. Designers perform this analysis to ensure that nominal designs function whenever the actual designs meet their tolerance specifications.

The kinematic function of a system is the coupling between its part motions due to contacts between pairs of parts. A lower pair has a fixed coupling that can be modeled as a permanent contact between two surfaces. For example, a revolute pair is modeled as a cylinder that rotates in a cylindrical shaft. A higher pair imposes multiple couplings due to contacts between pairs of part features. For example, gear teeth consist of involute patches whose contacts change as the gears rotate. The system transforms driving motions into outputs via sequences of part contacts. Small part variations can produce large motion variations, can alter contact sequences, and can introduce failure modes, such as jamming, due to qualitative changes in kinematic function. A complete kinematic tolerance analysis must bound the motion variations and must detect possible failures.

The mathematical model for kinematic tolerance analysis is constrained nonlinear optimization. The constraints specify the allowable part variations in terms of tolerance parameters with range limits. The objective function maps a part variation to the resulting kinematic variation. The maximum of this function is the worst-case kinematic variation. Computing the maximum is difficult because the objective function is an implicit function of the tolerance parameters and because there are many parameters. One solution is to linearize the objective function. The rationale is that nonlinear effects are insignficant because the tolerance parameters have narrow ranges. But this rationale is contradicted by tests on common higher pairs, such as cams, gears, and ratchets. The tests show that the linearization error reaches 100% and that failure modes are missed. Monte Carlo methods are another option, but they appear impractical for commercial applications because of the large number of tolerance parameters.

Higher pairs are especially hard to analyze because a separate optimization is required for every feature contact. Typical pairs have tens of feature contacts, and hundreds of contacts are common. Each contact involves distinct part features that depend on the parameters in a unique, nonlinear way. The analyst must compute the variation of every contact then combine the results to derive the variation of the pair. The situation is much worse in systems of higher pairs because the number of system contacts is the product of the number of pair contacts. Prior work does not provide analysis algorithms that handle general higher pairs or that detect failure modes.

We have developed a kinematic tolerance analysis algorithm that addresses these issues. The input is a parametric model of a planar system, parameter range limits, and nominal system configurations. The algorithm consists of two steps. The first step computes the kinematic variation of each pair at every contact configuration. The variation is represented in a geometric format, called a contact zone, that generalizes our configuration space representation of kinematic function [1] to toleranced parts. The contact zones also reveal qualitative changes in kinematic function. The second step estimates the worst-case system variation at the input system configurations by composing the contact zones. Contact zones are constructed and composed by novel forms of constrained optimization. We have tested the algorithm on mechanical systems comprised of common higher pairs. Extensive testing shows that the algorithm is more accurate than linearization, detects more failures, and solves large problems in under one minute.

The rest of the paper is organized as follows. Section 2 reviews prior work on kinematic tolerance analysis. Section 3 describes the configuration space representation of kinematic function. Sections 4–6 describe the kinematic tolerance analysis algorithm. Section 7 contains results from five industrial test cases. Section 8 contains a summary and plans for future work.

2 Prior work

Mechanical systems are toleranced for function and for assembly. Kinematic tolerance analysis is the most important aspect of functional tolerance analysis because kinematic function largely determines overall function. Other factors that effect function include inertia, stress, and deformation. The purpose of assembly tolerance analysis is to ensure that the parts of a system assemble despite manufacturing variation. The tolerance models and the analysis methods are very different from those of functional tolerancing, hence need not be surveyed here.

Prior work on kinematic tolerance analysis of mechanical systems falls into three increasingly general categories: static (small displacement) analysis, kinematic (large displacement) analysis of fixed contact systems, and kinematic analysis of systems with contact changes.

Static analysis of fixed contacts, also referred to as tolerance chain or stack-up analysis, is the most common. It consists of identifying a critical dimensional parameter (a gap, clearance, or play), building a tolerance chain based on part configurations and contacts, and determining the parameter variability range using vectors, torsors, or matrix transforms [2, 3]. Recent research explores static analysis with contact changes [4, 5, 6]. Configurations where unexpected failures occur can easily be missed because the software leaves their detection to the user.

Kinematic analysis of systems with fixed part contacts (mostly lower pairs) has been thoroughly studied in mechanical engineering [7]. It consists of defining kinematic relations between parts and studying their kinematic variation [8]. Commercial computer-aided tolerancing systems include this capability for planar and spatial mechanisms [9]. The kinematic variation is computed by linearization, which can be inaccurate, or by Monte Carlo simulation, which can be slow. Glancy and Chase [10] describe a hybrid algorithm that computes the first two derivatives of the system function with respect to the tolerance variables, calculates the first four moments of the system function, and fits an empirical variation distribution. This type of analysis is inappropriate for systems with many contact changes, such as the examples in this paper. The user must enumerate the contact sequences, analyze them with the software, compose the results, and detect failures.

We [11] developed the first kinematic tolerance analysis algorithm for systems with contact changes. That research introduces contact zones for modeling kinematic variation in higher pairs

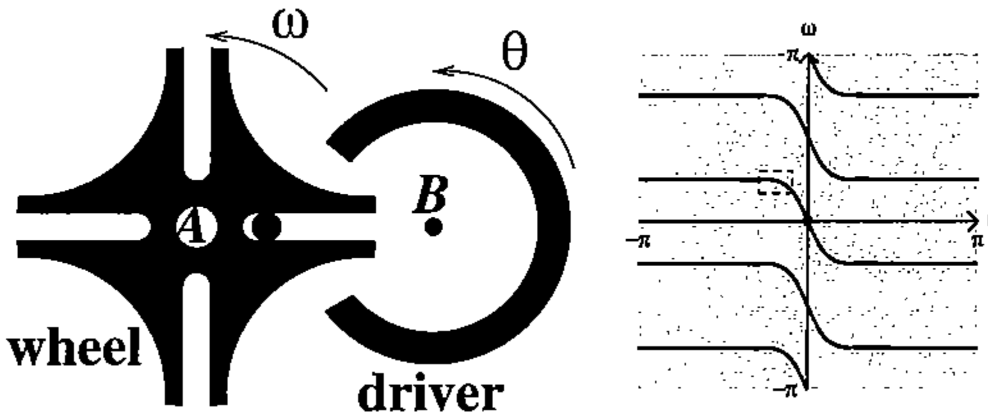

Figure 1: Geneva pair and its configuration space.

and composition for modeling system variation. The zones are computed and composed by linearization. This paper presents superior, nonlinear construction and composition algorithms.

3 Configuration space

We perform kinematic tolerance analysis within our configuration space representation of kinematics [12, 1]. The configuration space of a pair is a manifold with one coordinate per part degree of freedom (rotation or translation). Points in configuration space correspond to configurations of the pair. The configuration space partitions into blocked space where the parts overlap, free space where they are separate, and contact space where they touch. Free and blocked space are open sets whose common boundary is contact space. Contact space is a closed set comprised of curves that represent contacts between part features.

We illustrate these concepts on a Geneva pair comprised of a driver and a wheel (Figure 1). The driver consists of a driving pin and a locking arc segment mounted on a cylindrical base (not shown). The wheel consists of four locking arc segments and four slots. The wheel rotates around axis A and the driver rotates around axis B. Each driver rotation causes an intermittent wheel motion with four drive periods where the driver pin engages the wheel slots and with four dwell periods where the driver locking arc engages the wheel locking arcs.

The configuration space coordinates are the part orientations θ and ω in radians. The pair is displayed in configuration $(0, 0)$, which is marked with a dot. Blocked space is the grey region, contact space is the black curves, and free space is the channel between the curves. (Free space is invisible here, but appears as the white regions in Figures 5 and 6.) Free space forms a single channel that wraps around the horizontal and vertical boundaries, since the configurations at $\pm\pi$ coincide. The defining equations of the channel boundary curves express the coupling between the part orientations. The horizontal segments represent contacts between the locking arcs, which

Input: system, $\mathbf{u}_0$, $\mathbf{u}_l$, $\mathbf{u}_h$, tol, configurations.
1. Construct $\mathbf{u}_0$ configuration spaces.
2. Construct $[\mathbf{u}_l, \mathbf{u}_h]$ contact zones.
3. Compose contact zones at configurations.
Output: Contact zones and system variations.

Figure 2: Kinematic tolerance analysis algorithm.

hold the wheel stationary. The diagonal segments represent contacts between the pin and the slots, which rotate the wheel. The contact sequences of the pair are the configuration space paths in free and contact space. In a typical sequence, the driver rotates clockwise (decreasing θ) and alternately drives the wheel counterclockwise with the pin (increasing ω) and locks it with the arcs (constant ω).

4 Kinematic tolerance analysis algorithm

We analyze systems of planar higher pairs with parametric tolerances. A system is specified in a parametric boundary representation. The part profiles are simple loops of line and circle segments. Line segments are represented by their endpoints and circle segments are represented by their endpoints and radii. Each part translates along a planar axis or rotates around an orthogonal axis. The segment endpoints, circle radii, and motion axes are represented with algebraic expressions whose variables are tolerance parameters. This class of higher pairs covers 90% of engineering applications based on our survey of 2,500 mechanisms in an engineering encyclopedia [12] and on our industrial experience.

Figure 2 shows the kinematic tolerance analysis algorithm. The inputs are a parametric mechanical system, a vector $\mathbf{u}_0$ of initial parameter values, vectors $\mathbf{u}_l$ and $\mathbf{u}_h$ of lower and upper parameter range limits, a tolerance (10^{-5} in the examples), and a list of system configurations. The algorithm consists of three steps: configuration space construction, contact zone construction, and contact zone composition. Step 1 is described elsewhere [1]. The next two sections describe steps 2 and 3, which are the technical contribution of this paper.

5 Contact zone construction

We model kinematic variation by generalizing configuration space to parametric parts with tolerances. Kinematic variation occurs in contact space. As the parameters vary, the part shapes and motion axes vary, which causes the contact curves to vary. The union of the varying contact curves over the parameter range defines a band around the nominal contact space, called a contact zone, that bounds the worst-case kinematic variation of the pair. In other words, the contact zone is the

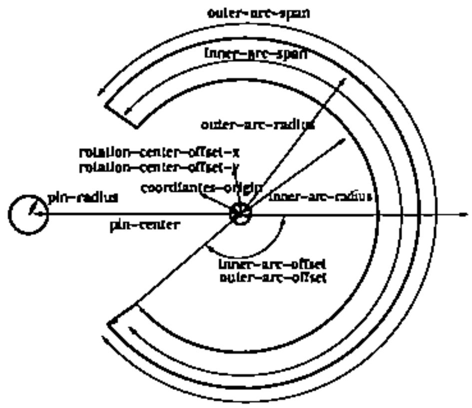

parameter	value
pin-radius	4.5mm
pin-center	56.5mm
outer-arc-radius	46.0mm
outer-arc-span	283.0°
outer-arc-offset	141.5°
inner-arc-radius	36.0mm
inner-arc-span	283.0°
inner-arc-offset	141.5°
rotation-center-offset-x	80.0mm
rotation-center-offset-y	0.0mm

Figure 3: Parametric model of Geneva driver.

subset of the configuration space where contacts can occur for some parameter variation. Hence, kinematic tolerance analysis is equivalent to contact zone construction.

Figure 5a shows the contact zone that our algorithm generates for the 26 parameter model of the Geneva pair shown in Figures 3 and 4 with parameter tolerances of ±0.02mm and $\pm 1^\circ$. The zone is a detail of the portion of the configuration space in the dashed box in Figure 1. This portion is the interface between a horizontal and a diagonal channel where the driver pin leaves a wheel slot and the locking arcs engage. The two dark grey bands that surround the channel boundary curves are the contact zone. The white region between the bands is the subset of the nominal free space that is free for all parameter variations.

The contact zone reveals that the part variations can cause the pair to jam. The lower and upper bands overlap near where the horizontal and diagonal channels meet. The overlap means that some parameter variations cause the two contacts to occur simultaneously, which yields a configuration space in which the channel is blocked (Figure 6b). Figure 6a shows the jamming configuration: the driver arc touches a wheel arc, which prevents the driver pin from leaving the wheel slot.

Figure 7 shows the contact zone construction algorithm. The inputs are a configuration space, nominal parameter values, and range limits. A separate zone is constructed for each contact curve in the configuration space. The curve is represented by a sequence of points such that the resulting piecewise linear curve approximates the contact curve to the input tolerance [1]. Steps 1 and 2 of the algorithm compute the variation at each curve point and step 3 links the results into a curve contact zone. The output is a list of these zones.

Step 1 formulates a parametric equation $C(\mathbf{p}, \mathbf{u}) = 0$ for a contact curve where $\mathbf{p}$ denotes the configuration space coordinates, for example $\mathbf{p} = (\theta, \omega)$ in the Geneva pair. There is one type of equation for every combination of features and motions, such as rotating circle/translating line. For example, the driver/wheel locking arc equation is $(B + R_\theta m - A - R_\omega n)^2 = (r - s)^2$ where B, A are the centers of rotation, m, n are the arc centers in part coordinates, R_θ, R_ω are rotation

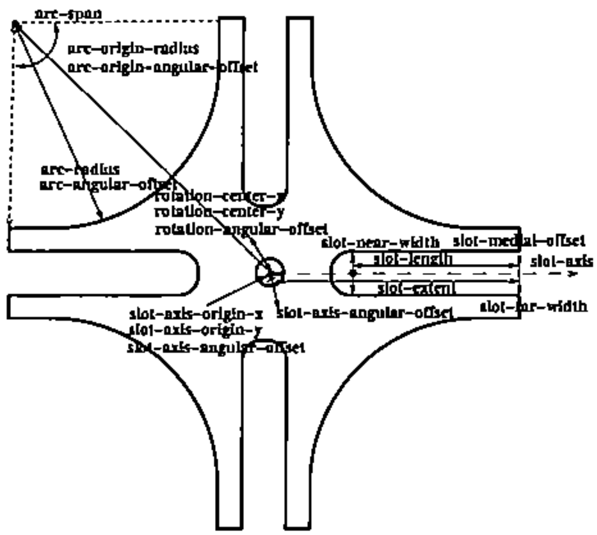

parameter	value
slot-axis-origin-x	0.0mm
slot-axis-origin-y	0.0mm
slot-axis-angular-offset	0.0°
slot-extent	60.0mm
slot-length	4.0mm
slot-medial-offset	0.0mm
slot-near-width	10.0mm
slot-far-width	10.0mm
arc-origin-radius	80.0mm
arc-origin-angular-offset	0.0°
arc-radius	46.68mm
arc-angular-offset	0.0°
arc-span	90.0°
rotation-center-x	0.0mm
rotation-center-y	0.0mm
rotation-angular-offset	0.0°

Figure 4: Parametric model of Geneva wheel.

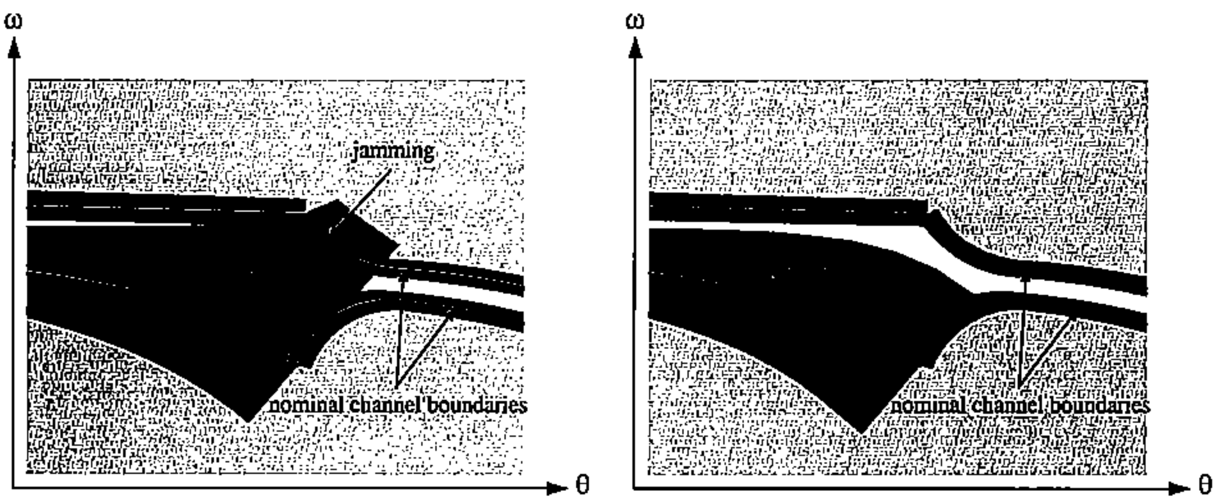

(a) (b)

Figure 5: (a) Detail of Geneva pair contact zone; (b) linear zone.

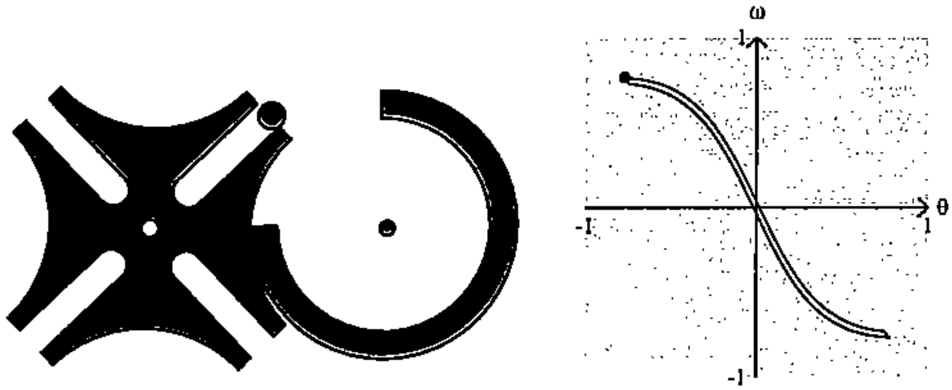

Figure 6: Jamming Geneva pair and its configuration space.

Input: cspace, $\mathbf{u}_0$, $\mathbf{u}_l$, $\mathbf{u}_h$.
For each contact curve
1. Formulate parametric contact equation.
2. Generate variation at curve points.
3. Form curve zone and add it to output.

Output: Contact zone.

Figure 7: Contact zone construction algorithm.

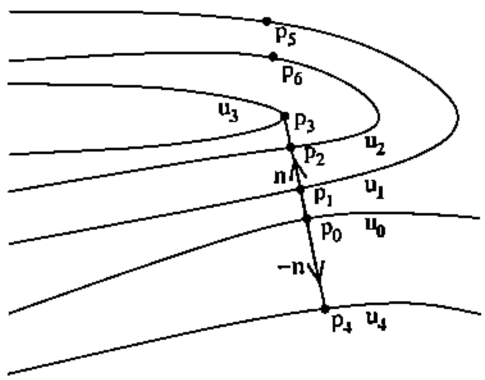

Figure 8: Kinematic variation.

operators, and r, s are the arc radii. The equation states that the distance between the arc centers equals the difference of their radii. The complete list of equations appears elsewhere [1].

Step 2 computes the worst-case kinematic variation at a nominal configuration $(\mathbf{p}_0, \mathbf{u}_0)$ on a contact curve. The variation is the maximum distance that the curve can move in an orthogonal direction (Figure 8). The variation occurs in the direction $\mathbf{n} = \pm C_\mathbf{p}/||C_\mathbf{p}||$ where $C_\mathbf{p}$ denotes $\partial C/\partial \mathbf{p}$ and is evaluated at $(p_0, \mathbf{u}_0)$. The two $\mathbf{n}$ values yield points on the upper and lower boundaries of the contact zone. The variation for $\mathbf{u} = \mathbf{u}_i$ is the first intersection of the line $p = p_0 + k\mathbf{n}$ with the contact curve $C(p, \mathbf{u}_i) = 0$, which is the smallest positive root of $f(k, \mathbf{u}_i) = C(\mathbf{p}_0 + k\mathbf{n}, \mathbf{u}_i)$. Later intersections are not reachable (lie outside the contact zone) because they are blocked by the first intersection. Figure 8 shows the first intersections for $\mathbf{u}_1, \ldots, \mathbf{u}_4$, which define the variations $p_1, \ldots, p_4$, and the second intersection p_5 and p_6 with the $\mathbf{u}_1$ and $\mathbf{u}_2$ curves. The worst-case variation is the maximum k for $\mathbf{u}$ in the parameter range.

Computing k is a nonstandard optimization problem: find a $\mathbf{u}$ that maximizes the smallest positive k such that $f(k, \mathbf{u}) = 0$ subject to the parameter range limits. There are two types of local maxima. Type 1 occurs when $f_k \neq 0$ and $f_\mathbf{u} = 0$. We can solve $f(k, \mathbf{u}) = 0$ for $k = g(\mathbf{u})$ with $\nabla g = -f_\mathbf{u}/f_k$ in a neighborhood of this point by the implicit function theorem. The point is an extremum of g because $\nabla g = 0$. Type 2 occurs when $f_k = 0$, for example p_3 in Figure 8. The chain rule shows that $\mathbf{n} \cdot C_\mathrm{p} = 0$, which means that the line $\mathbf{p}_0 + k\mathbf{n}$ is tangent to the $\mathbf{u}$ contact curve. Every nearby $\mathbf{u}$ value yields a curve that either does not intersect the line or whose first intersection is before k.

Figure 9 shows our algorithm for computing k via a sequence of line searches in $\mathbf{u}$. Step 1 initializes $\mathbf{u} = \mathbf{u}_0$ and $k = 0$. Step 2 tests for the two types of maxima. Steps 3–8 search the line $\mathbf{u} + t\nabla g$ for the first maximum of k in the positive t direction. This line is chosen because g increases most rapidly in the ∇g direction. The plane curve $h(t, s) = f(k + s, \mathbf{u} + t\nabla g) = 0$ is traced by the homotopy continuation method [13]. Step 3 starts the curve at $(t_0, s_0) = (0, 0)$ and steps 4–5 generate a sequence of points (t_i, s_i). The gradient search direction ensures that t and s are increasing at $t = 0$. The sequence ends at step 6 when the curve begins to decrease in s or t. At s turning points, a type 1 s maximum occurs between points $i - 1$ and i and is found by Newton iteration on $h = 0, h_t = 0$. At t turning points, a type 2 maximum is found by solving $h = 0, h_s = 0$. Step 7 updates k and $\mathbf{u}$ and the current line search ends. In the t case, the algorithm exits because $f_k = h_s = 0$.

The line search ends when the first maximum is found. Although other maxima could occur further along h, this is unlikely because tolerance parameters normally have narrow ranges. It is better to rely on later line searches to find such maxima (none of which have been observed to date). If the line reaches a range limit of parameter p_i, the ith term of ∇g is set to zero for the remainder of the line search, which is equivalent to treating p_i as a constant.

Our prior algorithm [11] linearizes f around $(0, \mathbf{u}_0)$ to obtain $kC_\mathbf{p} \cdot \mathbf{n} + C_\mathrm{u} \cdot (\mathbf{u} - \mathbf{u}_0) = 0$ then uses linear programming to maximize k subject to this equality and to the parameter range. Figure 5b shows the results for the Geneva pair. The linear zone is mostly accurate, but the lower band is much too narrow near where the channels meet. The quantitative error leads to the quali-

Input: f, $\mathbf{u}_0$, $\mathbf{u}_l$, $\mathbf{u}_h$.
1. Set $\mathbf{u} = u_0$; $k = 0$.
2. If $f_k = 0$ or $f_{\mathbf{u}} = 0$ return.
3. Set $s = 0; t = 0; i = 0; \nabla g = -f_{\mathbf{u}}/f_k$.
4. Set $i = i + 1$ and compute (t_i, s_i).
5. If $t_{i-1} < t_i$ and $s_{i-1} < s_i$ goto 4.
6. If $s_{i-1} > s_i$ solve $\{h = 0; h_t = 0\}$
   else solve $\{h = 0; h_s = 0\}$.
7. Set $k = k + s; \mathbf{u} = \mathbf{u} + t\nabla g$.
8. Goto 2.
Output: $\mathbf{u}$, k.

Figure 9: Algorithm for computing k.

tative error that the channel is always open, hence that jamming cannot occur. This type of error motivates the nonlinear algorithm, which produces the accurate zone shown in Figure 5a.

6 Contact zone composition

The final step in kinematic tolerance analysis estimates the kinematic variation of a system in an input configuration. Suppose that an input drives part A, which drives part B, which drives part C. The A/B contact zone yields the interval of possible B values at the input A configuration. The B/C zone yields the C variation at each B configuration in this interval. The algorithm composes these results to bound the interval of possible C configurations at the input system configuration. The optimization problem is to find $\mathbf{u}$ values that maximize and minimize $z = g(y, \mathbf{u})$ subject to $y = f(x_0, \mathbf{u})$ and to the range limits. Here $f(x, \mathbf{u})$ is the A/B contact curve, $g(y, \mathbf{u})$ is the B/C curve, and x_0 is the nominal x value. An arbitrary length chain of parts is composed via an analogous optimization.

Composition can be performed by a generalization of the algorithm for computing k in the previous section, but this approach is complicated and slow. We prefer to compute a bounding interval for the system variation by fast, simple methods. The upper bound is obtained by interval arithmetic: the z variation at x_0 is bounded by the union of the z variations at y over the y variation at x_0. The y variation at x_0 is the intersection interval, $[y_1, y_2]$, of the line $x = x_0$ with the A/B contact zone. The z variation over this interval is the intersection of the rectangle $y_1 \leq y \leq y_2$ with the B/C contact zone.

Interval arithmetic can overestimate the z variation when f and g share tolerance parameters. The maximum f and g variations cannot occur together, since one occurs at u_f and the other occurs at u_g, but interval arithmetic assumes that they can. A lower bound is obtained by heuristic parameter space sampling. The line segment (u_f, u_g) is sampled at a moderate number of points

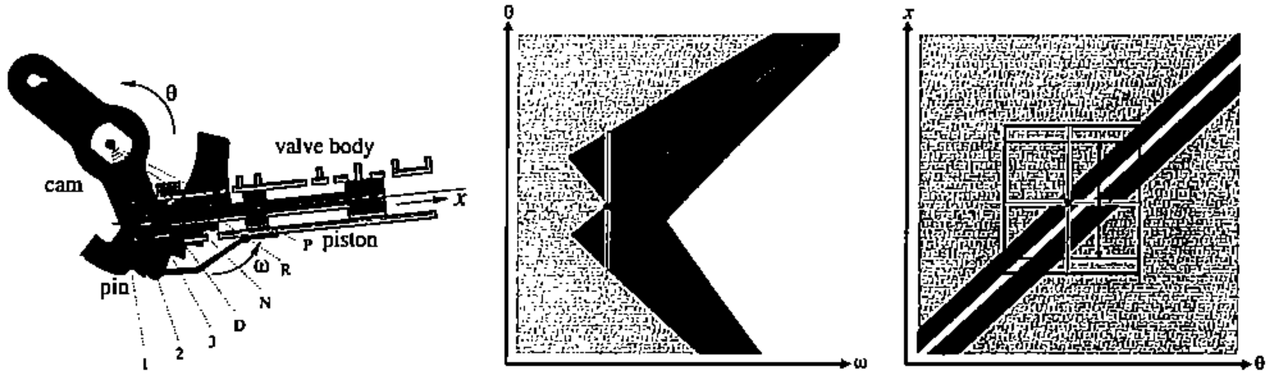

(a) (b) (c)

Figure 10: (a) Gear selector; (b) pin/cam contact zone; (c) cam/piston contact zone.

(10 in our examples), z is computed at each sample point, and the maximum is returned. The minimum of z is estimated in the same way.

We illustrate composition on a gear selector that we analyzed with Ford motors engineers [14]. The mechanism consists of a cam, a pin, a piston, and a fixed valve body (Figure 10a). The pin rotates around an attachment point on the valve body and is spring loaded. The piston translates along the valve body axis. The cam rotates around an axis at its center and is coupled to the piston. The driver rotates the cam into one of the seven gear settings (1, 2, 3, D, N, R, P) with a gearshift (not shown) then releases the gearshift. The pin rotates clockwise, engages in a triangular cavity in the cam bottom, and locks the cam into the current setting. In each setting, the piston closes prescribed conducts on the valve body, which govern motor function.

The kinematic tolerance analysis task is to determine the maximum variation of the piston displacement at each cam setting. Excessive variation can cause the piston to open the wrong conducts. The input motion drives the pin, which drives the cam, which drives the piston. Figures 10b and 10c show details of the pin/cam and cam/piston contact zones for a 33 parameter model with tolerances of ± 0.2 mm. The nominal pin/cam configuration is the intersection point of two diagonal contact curves that represent contacts between the pin and the sides of a cam cavity. The cam variation is marked by a vertical line segment through this configuration. The nominal cam/piston configuration lies on the upper boundary of a channel that represents coupled motion. The upper variation of the piston (1mm) is marked by a vertical line segment and the lower variation, (0.83mm) is marked by a double arrow. The black box illustrates the definition of the upper piston variation. The box width is the cam variation at ω_0 from the pin/cam contact zone. The box height is the union of the x variations in the cam/piston zone over the θ variations in the pin/cam zone.

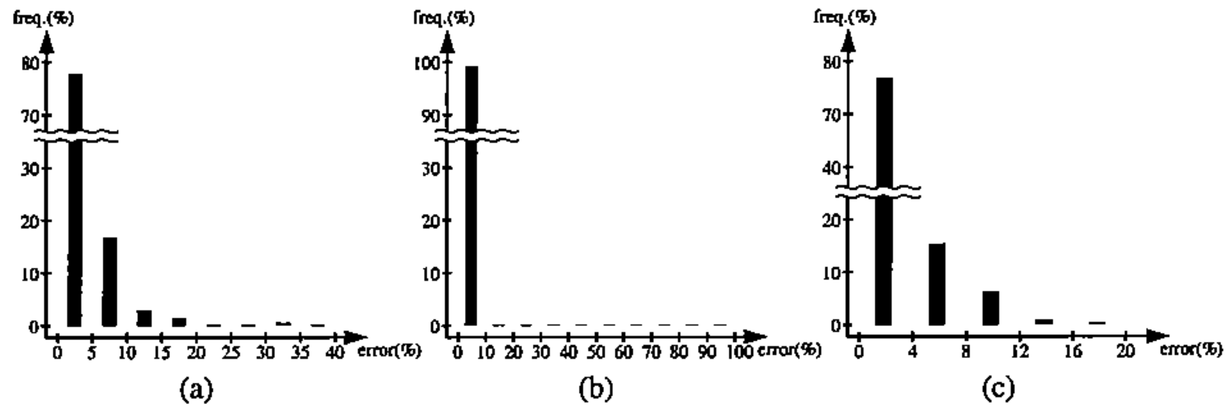

Figure 11: Linear contact zone error: (a) Geneva; (b) optical filter; (c) torsional ratcheting actuator.

7 Results

We have tested the kinematic tolerance analysis algorithm on representative mechanical systems from the engineering literature and from our collaboration with designers. Manual analysis and other analysis algorithms are impractical for these systems because they have many contacts, contact sequences, and tolerance parameters. Part of the testing is a comparison with the linear algorithm. We quantify the linear algorithm error as $(|a-c|+|b-d|)/|a-b|$ with $[a,b]$ the nonlinear variation and with $[c,d]$ the linear variation.

The first example is the Geneva pair. We have seen that the algorithm detects a failure mode that the linear algorithm misses. Figure 11a shows the relative error of the linear algorithm for our tolerances of ± 0.02mm and $\pm 1°$. The error is under 2% at 98% of the contact zone sample points, but is 36% on the lower channel boundary in the jamming region. The average error is 4%. The error for tolerances ± 0.01mm and $\pm 0.5°$ is always under 5%, which shows that linearization breaks down as the tolerances grow. The running time is 4.4 seconds CPU time on a Pentium 3 uniprocessor, versus 0.03 seconds for the linear algorithm. The contact zone consists of 60 contact curves, each with a different nominal kinematics and kinematic variation.

The second example is a cam/follower pair from an optical filter mechanism developed by Israel Aircraft Industries (Figure 12a). The parts are attached to a fixed frame with pin joints. Rotating the cam counterclockwise causes its pin to engage the follower slot and drive the follower clockwise. The follower motion ends when the cam pin leaves the slot, at which point the follower filter covers the lens. As the cam continues to rotate, its locking arc aligns with the complementary follower arc and locks the follower in place. Rotating the cam clockwise returns the filter to the initial state.

The configuration space shows correct nominal function (Figure 12b). The cam drives the follower in the diagonal channel and locks it in the horizontal channels. The contact zone is for a model with 23 parameters (Figure 12c). The upper detail shows that the upper portion of the

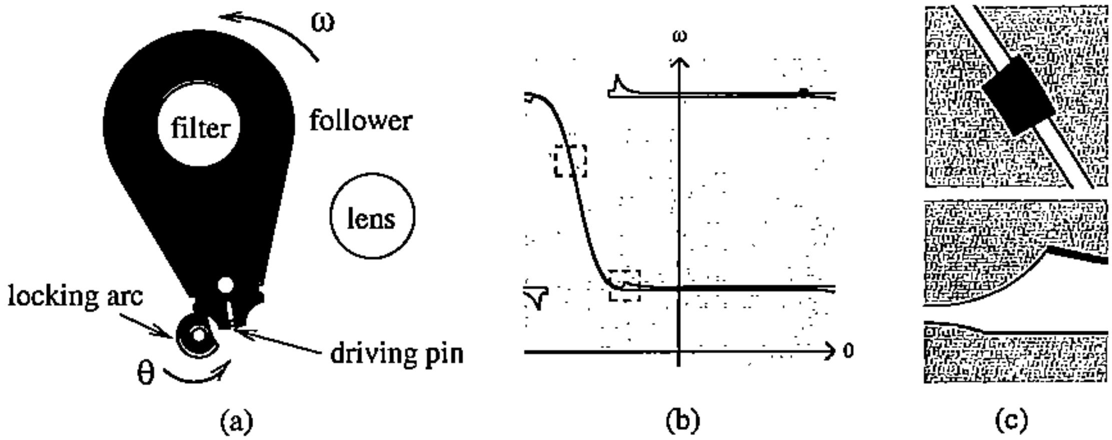

Figure 12: (a) Optical filter pair; (b) contact zone; (c) two details.

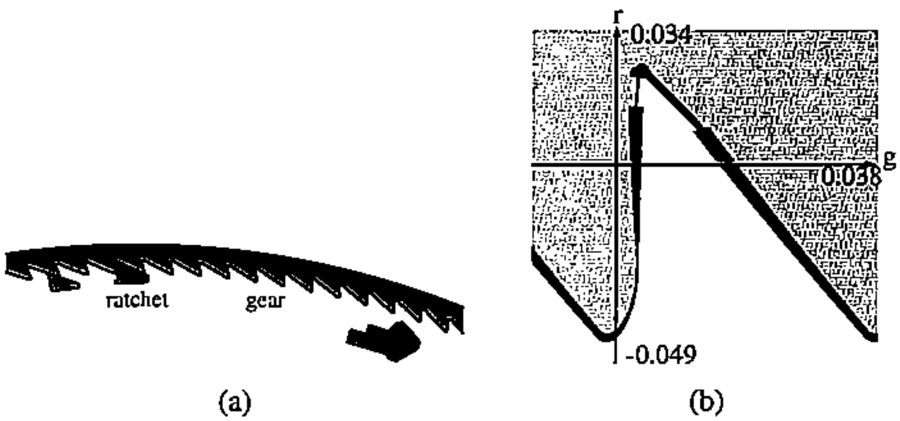

Figure 13: (a) Gear/ratchet pair; (b) contact zone.

diagonal channel can close, hence that the pair can jam. The lower detail shows that the interface between the diagonal and horizontal channels cannot close. The linear zone has 1% average error and a 100% maximum error (Figure 11b). The running time is 6 seconds versus 0.03 seconds for the linear algorithm. The contact zone consists of 34 contact curves.

The third example is a gear/ratchet pair from a torsional ratcheting actuator: a micro electro-mechanical system (MEMS) developed at Sandia National Laboratory [15, 16] (Figure 13a). The ratchet is attached to a driver (not shown) that is attached to the substrate by springs that allow planar rotation, but prevent translation. The driver is rotated counterclockwise by an electrostatic comb drive, which causes the ratchet to engages the inner teeth of the gear and rotate it counterclockwise. When the drive voltage drops, the springs restore the driver to its start orientation, which disengages the ratchet. The other parts are irrelevant to our discussion.

The contact zone reveals a design flaw (Figure 13b). The configuration space coordinates are

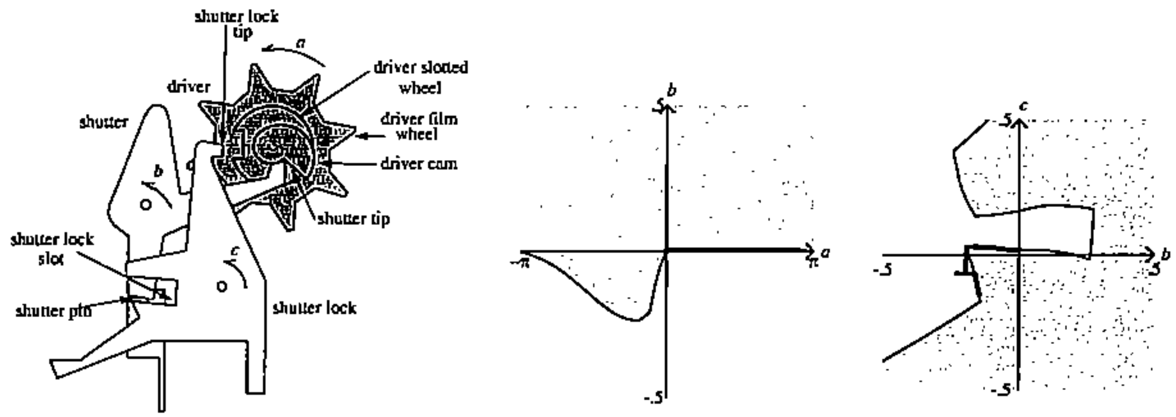

(a) (b) (c)

Figure 14: (a) Camera shutter mechanism; (b) driver/shutter configuration space; and (c) shutter/lock configuration space with motion path.

the gear orientation g and the ratchet orientation r. The dot marks the displayed configuration where the ratchet is driving the gear. The near vertical contact curve to the left represents the contact between the short side of a gear tooth and the ratchet tip, which prevents the gear from rotating clockwise relative to the driver. The contact zone shows that the near vertical curve can have a positive slope. When this happens, the gear can rotate clockwise, escape the ratchet, and jump to the next tooth. Friction will prevent this until the driver torque reaches a critical value that decreases as the kinematic variation increases. The detail also shows large variation in the diagonal curve to the right of the dot, but there is no qualitative impact because the slope is always negative.

The nonlinear zone is more accurate than the linear zone, which has 3% average error and 19% maximum error (Figure 11c). Both algorithms detect the failure mode. The running time is 2 seconds versus 0.01 seconds for the linear algorithm. The model has 18 tolerance parameters and the contact zone consists of 10 contact curves.

The fourth example is the gear selector. The average error of the linear zone is 1.5% and the maximum error is 22% for the cam/pin pair. The maximum occurs when the pin crosses between the triangular cam cavities. The average error is 0.2% and the maximum error is 2% for the cam/piston pair. The errors are near the averages in the seven cam settings. The error in the upper system variation is at most the distance between it and the lower variation. It ranges from 15% to 30% in the seven cam settings. The running time is 7 seconds versus 0.5 seconds for the linear algorithm. The model has 33 parameters and the contact zones consist of 31 contact curves.

The final example is a camera shutter mechanism comprised of a driver, a shutter, and a shutter lock (Figure 14a). The nominal function is as follows. The user advances the film (not shown), which engages the driver film wheel and rotates the driver counterclockwise. The shutter tip follows the driver cam profile, which rotates the shutter clockwise (Figure 14b), which extracts the

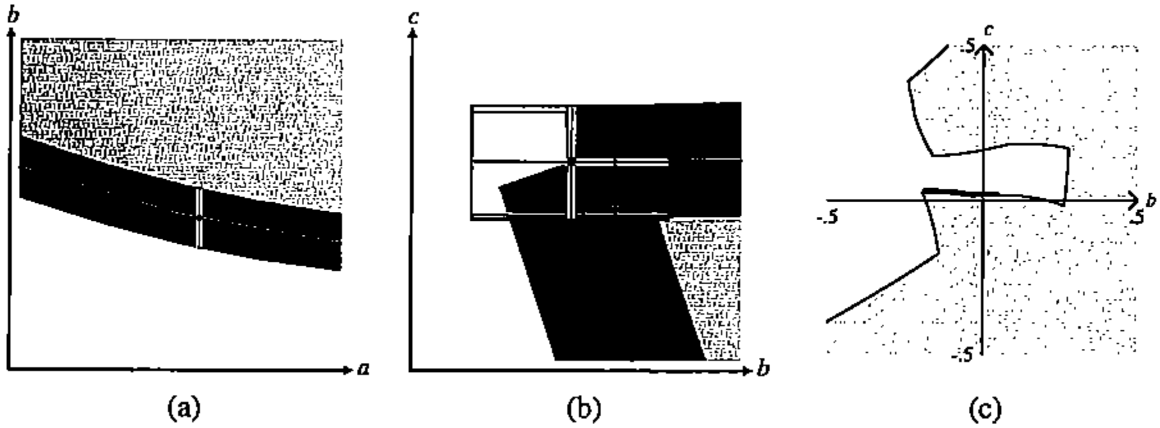

Figure 15: (a) driver/shutter contact zone detail; (b) shutter/lock contact zone detail; (c) failure in shutter/lock configuration space.

shutter pin from the shutter lock slot (Figure 14c). When the pin leaves the slot, a torsional spring rotates the shutter lock clockwise until its tip engages the driver slotted wheel.

Figures 15a–b show contact zone details near the configuration where the shutter pin leaves the shutter lock slot. The average error of the linear zone is 0.6% and the maximum error is 17% for the driver/shutter pair. The average error is 0.5% and the maximum error is 5% for the shutter/shutter lock pair. The system variation is displayed at this configuration. The upper and lower variations of the shutter lock are 0.4° and 0.36°. The variation can cause the mechanism to fail because the shutter does not move far enough left to clear the shutter lock (Figure 15c). The running time is 56 seconds versus 2 seconds for the linear algorithm. The model has 23 tolerance parameters and the contact zones consist of 329 curves.

The five test cases show that the kinematic tolerance analysis algorithm analyzes higher pairs accurately and quickly. It provides quantitative error bounds and detects failure modes. The nonlinear algorithm is always much more accurate than the linear algorithm, as measured by the maximum error. The maximum error is the appropriate measure because an incorrect estimate at a single configuration can hide a failure mode, as shown in Figure 5.

8 Conclusions

We have presented a nonlinear kinematic tolerance analysis algorithm for planar mechanical systems of higher pairs with parametric tolerances. The algorithm constructs generalized configuration spaces, called contact zones, that bound the worst-case kinematic variation of the pairs over the tolerance parameter range. The zones specify the variation of the pairs at every contact configuration and reveal error modes, such as jamming. The algorithm bounds the system variation at a selected configuration by composing the zones of the touching parts. We have assessed the algorithm with case studies on common types of higher pairs. The algorithm produces accurate contact zones, detects failure modes, and greatly improves upon linearization.

We see several directions for future work. The contact zone construction and composition algorithms apply to systems of three-dimensional parts that move along spatial axes. We have developed the requisite configuration space construction algorithm [17]. We need to formulate parametric equations for every type of spatial contact, which is tedious, but straightforward. The other steps carry over from the planar algorithm. Contact zone construction extends to general planar pairs, which have three dimensional zones, following our linear algorithm [18]. Composition requires further research to address closed kinematic chains, which cannot arise in fixed-axis systems. Another research direction is to automate the detection of contact sequence changes and of qualitative changes in kinematic function, as in our higher pair synthesis algorithm [19].

Acknowledgments

This research was supported by NSF grants IIS-0082339 and CCR-9617600, the Purdue Center for Computational Image Analysis and Scientific Visualization, a Ford University Research Grant, the Ford ADAPT 2000 project, and grant 98/536 from the Israeli Academy of Science.

References

[1] Elisha Sacks and Leo Joskowicz. Computational kinematic analysis of higher pairs with multiple contacts. *Journal of Mechanical Design*, 117(2(A)):269–277, June 1995.

[2] André Clemént, Alain Rivière, Phillipe Serré, and Catherine Valade. The ttrs: 13 constraints for dimensioning and tolerancing. In *Proc. of the 5th CIRP Int. Seminar on Computer-Aided Tolerancing*, Toronto, 1997.

[3] Daniel Whitney, Olivier Gilbert, and Marek Jastrzebski. Representation of geometric variations using matrix transforms for statistical tolerance analysis. *Research in Engineering Design*, 6(4):191–210, 1994.

[4] Eric Ballot and Pierre Bourdet. A computation method for the consequences of geometric errors in mechanisms. In *Proc. of the 5th CIRP Int. Seminar on Computer-Aided Tolerancing*, Toronto, 1997.

[5] Jingliang Chen, Ken Goldberg, Mark Overmars, Dan Halperin, Karl Bohringer, and Yan Zhuang. Shape tolerance in feeding and fixturing. In P.K. Agarwal, L. E. Kavraki, and M. T. Mason, editors, *Robotics, The Algorithmic Perspective: 3rd Workshop on Algorithmic Foundations of Robotics (WAFR)*. A. K. Peters, 1998.

[6] Matsamoto Inui and Masashiro Miura. Configuration space based analysis of position uncertainties of parts in an assembly. In *Proc. of the 4th CIRP Int. Seminar on Computer-Aided Tolerancing*, 1995.

[7] G. Erdman, Arthur. *Modern Kinematics: developments in the last forty years*. John Wiley and Sons, 1993.

[8] Kenneth Chase, Spencer Magleby, and Charles Glancy. A comprehensive system for computer-aided tolerance analysis of 2d and 3d mechanical assemblies. In *Proc. of the 5th CIRP Int. Seminar on Computer-Aided Tolerancing*, Toronto, 1997.

[9] O.W. Solomons, F. van Houten, and H. Kals. Current status of cat systems. In *Proc. of the 5th CIRP Int. Seminar on Computer-Aided Tolerancing*, Toronto, 1997.

[10] Charles G. Glancy and Kenneth W. Chase. A second-order method for assembly tolerance analysis. In *Proceedings of the ASME Design Automation Conference*, 1999.

[11] Elisha Sacks and Leo Joskowicz. Parametric kinematic tolerance analysis of planar mechanisms. *Computer-Aided Design*, 29(5):333–342, 1997.

[12] Leo Joskowicz and Elisha Sacks. Computational kinematics. *Artificial Intelligence*, 51(1-3):381–416, October 1991. reprinted in [20].

[13] Alexander P. Morgan. *Solving Polynomial Systems Using Continuation for Scientific and Engineering Problems*. Prentice-Hall, Englewood Cliffs, NJ, 1987.

[14] Elisha Sacks, Leo Joskowicz, Ralf Schultheiss, and Uwe Hinze. Computer-assisted kinematic tolerance analysis of a gear selector mechanism with the configuration space method. In *25th ASME Design Automation Conference*, Las Vegas, 1999.

[15] Stephen M. Barnes, Samuel L. Miller, M. Steven Rodgers, and Fernando Bitsie. Torsional ratcheting actuation system. In *Third International Conference on Modeling and Simulation of Microsystems*, San Diego, CA, 2000.

[16] Elisha Sacks and Steven M. Barnes. Computer-aided kinematic design of a torsional ratcheting actuator. In *Proceedings of the Fourth International Conference on Modeling and Simulation of Microsystems*, Hilton Head, SC, 2001.

[17] Ku-Jim Kim, Elisha Sacks, and Leo Joskowicz. Kinematic analysis of spatial fixed-axis higher pairs using configuration spaces. Technical Report CSD-TR 02-001, Purdue University, 2002. To appear in *Computer-Aided Design*.

[18] Elisha Sacks and Leo Joskowicz. Parametric kinematic tolerance analysis of general planar systems. *Computer-Aided Design*, 30(9):707–714, August 1998.

[19] Min-Ho Kyung and Elisha Sacks. Parameter synthesis of higher kinematic pairs. Technical Report CSD-TR 01-020, Purdue University, 2001. To appear in *Computer-Aided Design*.

[20] K. Goldberg, D. Halperin, J.C. Latombe, and R. Wilson, editors. *The Algorithmic Foundations of Robotics*. A. K. Peters, Boston, MA, 1995.